AGU PUBLICATIONS

Geophysical Research Letters

RESEARCH LETTER
10.1002/2014GL059684

Key Points:
- Poor detectability of fossil fuel CO_2 emissions from subcontinental regions
- Detectability assessed via attribution of emissions patterns in atmospheric data
- Loss in detectability due to transport modeling errors and biospheric signal

Supporting Information:
- Readme
- Text S1
- Figure S1
- Figure S2
- Table S1
- Table S2
- Table S3

Correspondence to:
Y. P. Shiga,
yshiga@stanford.edu

Citation:
Shiga, Y. P., A. M. Michalak, S. M. Gourdji, K. L. Mueller, and V. Yadav (2014), Detecting fossil fuel emissions patterns from subcontinental regions using North American in situ CO_2 measurements, *Geophys. Res. Lett.*, *41*, 4381–4388, doi:10.1002/2014GL059684.

Received 21 FEB 2014
Accepted 30 MAY 2014
Accepted article online 5 JUN 2014
Published online 24 JUN 2014

This is an open access article under the terms of the Creative Commons Attribution-NonCommercial-NoDerivs License, which permits use and distribution in any medium, provided the original work is properly cited, the use is non-commercial and no modifications or adaptations are made.

Detecting fossil fuel emissions patterns from subcontinental regions using North American in situ CO_2 measurements

Yoichi P. Shiga[1,2], Anna M. Michalak[2], Sharon M. Gourdji[3], Kim L. Mueller[4], and Vineet Yadav[2]

[1]Department of Civil and Environmental Engineering, Stanford University, Stanford, California, USA, [2]Department of Global Ecology, Carnegie Institution for Science, Stanford, California, USA, [3]Department of Environmental and Earth Systems Science, Stanford University, Stanford, California, USA, [4]Science and Technology Policy Institute, Washington, District of Columbia, USA

Abstract The ability to monitor fossil fuel carbon dioxide ($FFCO_2$) emissions from subcontinental regions using atmospheric CO_2 observations remains an important but unrealized goal. Here we explore a necessary but not sufficient component of this goal, namely, the basic question of the detectability of $FFCO_2$ emissions from subcontinental regions. Detectability is evaluated by examining the degree to which $FFCO_2$ emissions patterns from specific regions are needed to explain the variability observed in high-frequency atmospheric CO_2 observations. Analyses using a CO_2 monitoring network of 35 continuous measurement towers over North America show that $FFCO_2$ emissions are difficult to detect during nonwinter months. We find that the compounding effects of the seasonality of atmospheric transport patterns and the biospheric CO_2 flux signal dramatically hamper the detectability of $FFCO_2$ emissions. Results from several synthetic data case studies highlight the need for advancements in data coverage and transport model accuracy if the goal of atmospheric measurement-based $FFCO_2$ emissions detection and estimation is to be achieved beyond urban scales.

1. Introduction

Independent evaluation of bottom-up inventory-based estimates of fossil fuel carbon dioxide ($FFCO_2$) emissions remains a critical yet challenging endeavor. At the global level, inventory-based $FFCO_2$ emissions estimates have relatively low uncertainty (<10%) [*Marland*, 2008]. These uncertainties rise, however, with increasing spatial and temporal resolution [*Marland*, 2008]. Uncertainties are also higher in regions with less sophisticated accounting methods [e.g., *Guan et al.*, 2012], which coincide with regions with the largest projected growth in $FFCO_2$ emissions. While increasingly sophisticated bottom-up methods have been developed [e.g., *Gurney et al.*, 2009, 2012; *Rayner et al.*, 2010; *Andres et al.*, 2011; *Oda and Maksyutov*, 2011; *Nassar et al.*, 2013], independent atmospheric observation-based evaluations of such approaches have not been conducted at subcontinental or national scales.

Verifying the accuracy of bottom-up $FFCO_2$ emissions estimates is critical both for constraining the behavior of the natural (i.e., biospheric and oceanic) components of the carbon cycle and for evaluating compliance with any agreements to manage $FFCO_2$ emissions. Atmospheric observation-based methods used to estimate the natural components of the carbon budget typically presubtract the FF component from the atmospheric observations under the assumption that $FFCO_2$ emissions estimates are well known. However, such an approach aliases errors in $FFCO_2$ emissions estimates onto the natural carbon cycle estimates [*Gurney et al.*, 2005; *Peylin et al.*, 2011] and does not provide a way of updating the $FFCO_2$ emissions estimates themselves. Additionally, discussions focusing on limiting future emissions would benefit from independent estimates of $FFCO_2$ emissions as a means of evaluating and verifying self-reported progress toward emissions reduction goals [*Pacala et al.*, 2010].

One clear approach for providing such independent verification [*Pacala et al.*, 2010] is atmospheric inverse modeling, a top-down approach that uses atmospheric concentration measurements coupled with an atmospheric transport model to infer fluxes from upwind locations. However, with current observational networks focused on constraining natural CO_2 fluxes, uncertainties in existing inverse modeling systems were quoted as being too large (>100%) to constrain continental or nation level $FFCO_2$ emissions [*Pacala et al.*, 2010].

©2014. The Authors.

Pacala et al. [2010] suggested several steps to reduce uncertainties in inverse estimates of $FFCO_2$ emissions at annual national levels to within 10–50%, including expanding remote sensing and in situ observations, deploying measurement capabilities for the radiocarbon isotope ^{14}C, and increasing the monitoring of large local (i.e., urban) sources. A multitude of efforts in line with these suggestions are currently underway (e.g., Hestia Project [*Gurney et al*., 2012], Indianapolis Flux Experiment (http://influx.psu.edu/), Megacities Carbon Project [*Duren and Miller*, 2012; *Kort et al*., 2012; *Miller et al*., 2012]) with a majority focusing on high-emitting urban areas. The recent shift in focus toward monitoring large emitting urban areas offers the benefits, among others, of reducing the interference of natural carbon fluxes and constraining ~75% of the global $FFCO_2$ budget [*Duren and Miller*, 2012]. However, scaling these efforts up from the urban scale to create subcontinental or national level $FFCO_2$ emissions estimates is likely not feasible.

Thus, exploring the capabilities and limitations of existing CO_2 monitoring networks in examining the $FFCO_2$ signal is critical to identify viable pathways toward the goal of $FFCO_2$ emissions quantification and monitoring. Further examination is vital to answer key questions within the current $FFCO_2$ monitoring paradigm (e.g., where/when $FFCO_2$ emissions are detectable and why/how is the detectability of $FFCO_2$ emissions limited). While it is clear that current atmospheric CO_2 monitoring networks were not designed to monitor $FFCO_2$ emissions, "the question of whether the amplitude of the greenhouse gas perturbations caused by national emissions is large enough to detect with in situ networks or satellites" [*Pacala et al*., 2010] remains to be answered. Although the ultimate goal is to quantify $FFCO_2$ emissions using atmospheric observations, it follows that if one cannot detect the $FFCO_2$ emissions signal, the more difficult task of quantification will likewise not be possible. In this study, we aim to investigate the detection of $FFCO_2$ emissions as a baseline requirement for the quantification and monitoring of $FFCO_2$ emissions.

Although "detectability" can have a variety of definitions, the notion as defined here focuses on the capacity to distinguish a pattern of interest ($FFCO_2$ emissions from a given region) amidst distracting or background patterns (e.g., natural CO_2 fluxes, atmospheric transport modeling errors, and aggregation errors) above a certain threshold, given a set of observations. In the work presented here, the threshold is defined as a statistical model selection problem, using the Bayesian Information Criterion (BIC) [*Schwarz*, 1978], a common tool for statistical model selection in multiple linear regression [*Ward*, 2008], as the basis for selection. Hence, detectability is analogous to the decision to include a given explanatory variable in a regression analysis, based on the criterion that the variable itself explains a substantial portion of the variability observed in available measurements. The central question in this work therefore focuses on the extent to which the variations in the atmospheric data can be attributed to patterns arising from $FFCO_2$ emissions (see section 2 and the supporting information for details).

North America (NA), with its expansion of continuous (high-frequency) in situ CO_2 measurements and the existence of two high-resolution $FFCO_2$ emissions inventories, VULCAN [*Gurney et al*., 2009] and Open-source Data Inventory for Anthropogenic CO_2 (ODIAC) [*Oda and Maksyutov*, 2011], offers an ideal experimental platform for this investigation. The in situ observations and the $FFCO_2$ emissions inventories were coupled with a high-resolution geostatistical inverse modeling framework [e.g., *Michalak et al*., 2004; *Gourdji et al*., 2012] to investigate the detectability of $FFCO_2$ emissions patterns in the observed CO_2 concentration signal.

We also investigated the influence of "distracting or background patterns," i.e., natural CO_2 fluxes and errors due to atmospheric transport modeling uncertainties, on detectability using several synthetic data experiments. In the synthetic data experiments, natural fluxes and simulated atmospheric transport model errors were "turned on" or "turned off" in order to characterize the specific causes for losses in detectability and in so doing inform avenues for improving detectability.

2. Detecting the $FFCO_2$ Signal

To investigate whether the spatiotemporal patterns of $FFCO_2$ emissions can be observed in the total CO_2 signal, z_{Total} (i.e., atmospheric observations), a realistic representation of $FFCO_2$ emissions was needed. This was created by merging two high-resolution $FFCO_2$ emissions inventory data sets, VULCAN version 2.0 [*Gurney et al*., 2009] over the contiguous U.S. and the ODIAC product [*Oda and Maksyutov*, 2011] over Canada, Mexico, and Alaska as in *Gourdji et al*. [2012]. The VULCAN-ODIAC merged inventory was then rescaled to $1° \times 1°$ spatial resolution and a three hourly temporal resolution (see supporting information for details). The

©2014. The Authors.

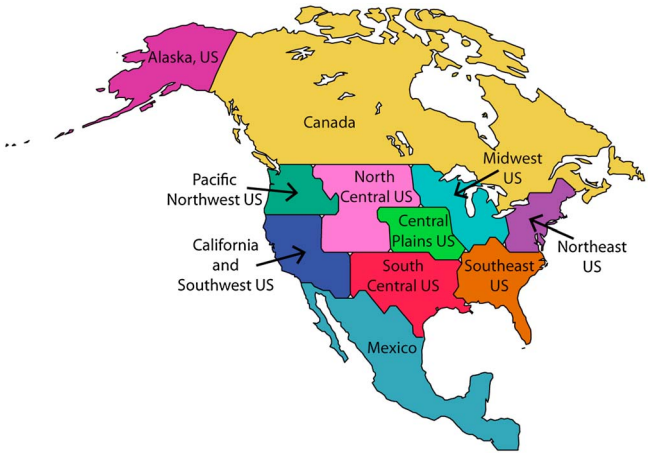

Figure 1. The 11 North American regions used in the model selection analysis. The contiguous United States are divided by EPA region, with "Northeast U.S." region created by merging EPA regions 1, 2, and 3.

merged VULCAN-ODIAC product was then transported forward to observation locations using the Stochastic Time-Inverted Lagrangian Transport model [*Lin et al*., 2003], driven by meteorological fields from the Weather Research and Forecast (WRF) model [*Skamarock and Klemp*, 2008]. Thus a 3 h temporal resolution observation vector, z_{FF}, was created containing the atmospheric signature resulting from the fine-scale spatiotemporal behavior of $FFCO_2$ emissions. The resulting analyses are based on the spatiotemporal patterns from the VULCAN-ODIAC $FFCO_2$ emissions product. For the synthetic data experiments, the FF signal was combined with a synthetic biospheric signal and simulated transport model errors, with the biospheric signal also being based on fluxes defined at $1° \times 1°$ spatial resolution and a three hourly temporal resolution (see supporting information for details).

We were interested in investigating not only if, but where and when $FFCO_2$ emissions patterns from subcontinental regions are observable. To explore this, we subdivided the $FFCO_2$ emissions from NA into 11 subcontinental regions: Mexico, Canada, and nine modified Environmental Protection Agency (EPA) regions for the U.S. (Figure 1). We define these regions as such because they represent political/policy-relevant domains and together encompass the entire NA continent. The 11 spatial regions were further subdivided by month and used to produce the resulting atmospheric $FFCO_2$ signals from these 132 region-months, z^i_{FF}. Note that we did not aggregate or average $FFCO_2$ emissions over these region-months but rather kept the fine-scale spatiotemporal patterns of $FFCO_2$ emissions intact within each of these space-time region-months. This was done in order to examine the ability of the variations in the CO_2 signal as seen by the atmospheric observation network to be attributed to the fine-scale spatiotemporal patterns in $FFCO_2$ emissions.

The detectability of each region-month was then assessed using a BIC-based model selection procedure that has been previously adapted to account for correlated residuals [*Mueller et al*., 2010] and for use in an inverse modeling system [*Gourdji et al*., 2012] (see supporting information for details). This BIC setup incorporates the information used in a typical atmospheric trace gas inverse model, i.e. the sensitivity of the observations to surface fluxes, the flux error covariances, and the model-data mismatch covariances, but we focused here only on identifying region-months that are detectable from the atmospheric observations, rather than on quantifying $FFCO_2$ emissions per se. The goal was to create a model that explained the variability in z_{Total} using a combination of z^i_{FF}, ensuring that each z^i_{FF} explains a sufficient portion of the variability in z_{Total}. We used BIC as an objective metric/threshold to determine which region-months were detectable, as BIC penalizes larger models and hence only considers $FFCO_2$ emissions from given region-months detectable if they sufficiently improve the model fit (equation (S1)). Because the $FFCO_2$ signal explains only a small portion of the total atmospheric CO_2 signal (Table S3) BIC helps to identify only those region-months of $FFCO_2$ emissions that substantially contribute to the variability observed in $\boldsymbol{z}_{Total}$ (see supporting information for details). Thus, the $FFCO_2$ emissions patterns from a given region-month are detected if the z^i_{FF} from that region-month is included in the model with the lowest BIC value.

3. Case Studies

Accurate detection of the $FFCO_2$ emissions signal from atmospheric measurements is hindered by several factors or "distracting patterns," including mixing of $FFCO_2$ fluxes with biospheric CO_2 fluxes, atmospheric transport model errors (including but not limited to: representation and aggregation errors), the heterogeneity and density of the measurement network, and errors in the spatiotemporal representation of

©2014. The Authors.

the $FFCO_2$ emissions signal. These factors are all inherently enmeshed in real atmospheric data but can be isolated when using synthetic data. Thus, several synthetic case studies were explored to better understand the factors that lead to diminishing detectability.

A real data (RD_BFE) case study was also explored, using atmospheric CO_2 measurements from 2008. High-frequency atmospheric CO_2 concentration data were collected from 35 towers located in the U.S. and Canada (Table S1). The four synthetic data (SD) case studies were developed to explore when, where, why, and how $FFCO_2$ emissions detectability diminished relative to an idealized case.

The synthetic data case studies used various combinations of biospheric fluxes (B) from CASA-GFEDv2 [*Randerson et al*., 1997; *van der Werf et al*., 2006], $FFCO_2$ fluxes (F) from VULCAN-ODIAC and simulated atmospheric transport model errors (E) optimized from the 2008 data (details of all components in the supporting information). For all of the SD cases, the $FFCO_2$ emissions used to create the FF component in the atmospheric data are also used to represent the spatiotemporal $FFCO_2$ emissions signal in the detectability analysis. The SD_BFE case combined biospheric (B) and FF (F) fluxes as well as simulated atmospheric transport model errors (E) to create the most realistic synthetic atmospheric data scenario. A comparison between SD_BFE and RD_BFE results was used to assess the ability to represent the complexity of the real data case, thus ensuring that subsequent deconstructed SD cases could be used to gain insights into the system.

The SD_ØFØ case represents an ideal case where only the $FFCO_2$ fluxes (F) are present, with no biospheric fluxes (Ø) or simulated atmospheric transport model errors (Ø). This case represents an idealized scenario where CO_2 could be treated as a perfect tracer for $FFCO_2$ emissions. To isolate the effects of the biospheric CO_2 signal on limiting detectability, the SD_BFØ case added only biospheric (B) fluxes to the ideal case. Likewise, the SD_ØFE case added only simulated transport model errors, with no biospheric fluxes, enabling an investigation into the effects of transport model errors on hindering detectability. The SD_BFE case was ultimately used to investigate the combined effects of the biospheric CO_2 signal and transport model errors on limiting detectability. Realistic data choices (identical to 2008 actual data availability) were used for all synthetic data cases.

4. Results of Detectability Analysis

4.1. $FFCO_2$ Detectability

We first examine the detectability of the $FFCO_2$ emissions signal over NA using the real data from 2008 (i.e., the RD_BFE case). The conceptual definition of detectability presented in section 1 is represented by the methodology described in section 2 and the supporting information. For the discussion that follows, the term "detected" specifies a region-month where the $FFCO_2$ emissions were selected through BIC (i.e., included in the model with the lowest BIC value).

We find that $FFCO_2$ emissions detectability is better during winter (higher percentage of regions detected) than spring, summer, and fall (Figure 2, first row). Alaska remains undetected throughout the year due to a lack of measurement coverage (Figure S1) and a relatively small $FFCO_2$ emissions signal. $FFCO_2$ emissions are detected during at least 6 months of the year in the Midwestern U.S., Northeastern U.S., and California and Southwest U.S. regions. It is clear that even with the extensive network in 2008, the simple goal of detecting, let alone quantifying, $FFCO_2$ emissions is challenging for a large portion of the continent over much of year. However, in certain regions (Midwestern U.S., Northeastern U.S., California, and Southwest U.S. regions) and during certain times of the year (winter) the variability in the atmospheric observations can be directly attributed to patterns consistent with $FFCO_2$ emissions.

4.2. Information Content of Observations

The SD_BFE case is intended to be a scenario that offers a realistic representation of reality and one in which, unlike the real data case, the $FFCO_2$ emissions are perfectly known. SD_BFE is thus compared to RD_BFE (Figure 2, first and second rows) to determine whether it realistically represents the complexity of a real data scenario. The detectability results of these two cases are found to have several similarities: both exhibit parallel spatial and seasonal patterns in $FFCO_2$ emissions detectability. In both cases, winter represents the only time when the detectability across much of the continent is possible, excluding Alaska and Mexico. In

©2014. The Authors.

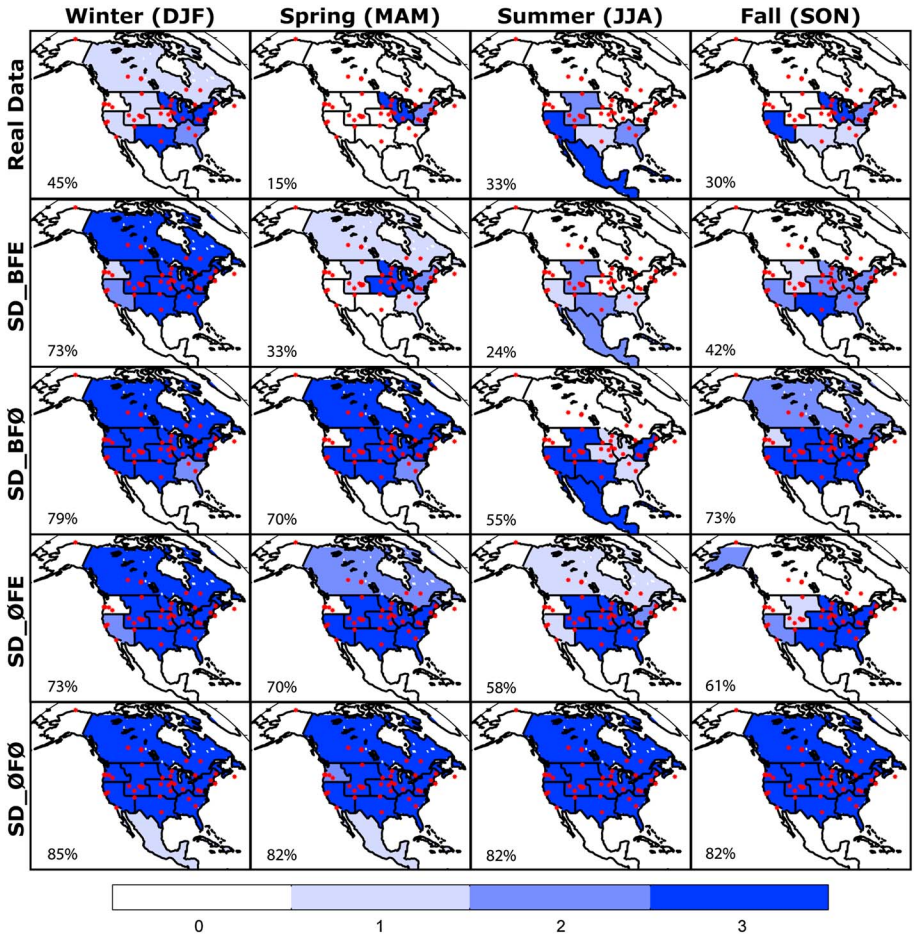

Figure 2. (first–fifth rows and first to fourth columns) Results of the model selection analysis by region and season. Colors represent the number of months per season (0 to 3) for which the FF emissions from a region are detectable. Red stars represent continuous observation locations for 2008. The percent of region-months detected per season (Number detected/33 total region-months × 100%) is also shown.

both cases, the regions detected during the summer months are the same: Mexico, South Central U.S., California and Southwest U.S., Southeast U.S., and North Central U.S. Several differences in the detectability results also exist, for instance, while detectability deteriorates in the spring, fall, and summer for both cases, the minimum detectability for the SD_BFE case occurs during the summer not spring as in the RD_BFE case. This may be due to incorrect timing of the growing season in the modeled biosphere or stronger and more variable biospheric activity in reality than in the model.

The results of the SD_BFE case demonstrate that the distracting patterns, rather than uncertainties in the inventory used in RD_BFE, are the main drivers of the loss in detectability. This result supports the use of the subsequent deconstructed synthetic data cases to investigate how various factors contribute to the lack of detectability.

4.3. Effect of Biospheric Fluxes on Detectability

The difference between the detectability results of the SD_ØFØ and SD_BFØ case studies (Figure 2, fifth and third rows) represents the impact of biospheric CO_2 fluxes and their seasonality on the detectability of $FFCO_2$ emissions. Because neither case includes simulated transport model errors, any loss in detectability from SD_ØFØ to SD_BFØ is due to the influence of biospheric fluxes.

The detectability in SD_ØFØ is limited only by the sensitivity of the atmospheric measurements to the underlying fluxes (Figure S1) and demonstrates that in the absence of any other confounding factors, $FFCO_2$ emissions are detectable in all regions except Alaska and Mexico throughout the year (Figure 2, fifth row). The

©2014. The Authors.

inclusion of the biospheric flux signal in SD_BFØ leads to a major loss in the detectability of $FFCO_2$ emissions during the summer (Figure 2, third row and third column). Detectability losses in the spring, fall, and winter are smaller. This result indicates that even without model-data mismatch errors due in large part to transport model uncertainties, the biospheric signal acts as a major confounding factor in the detection of the $FFCO_2$ signal during the summer months.

These results suggest that the use of additional tracers (e.g., radiocarbon isotope ^{14}C, carbon monoxide) [*Turnbull et al*., 2006, 2011; *Miller et al*., 2012] that help to isolate $FFCO_2$ emissions from biospheric would indeed help to improve detectability of $FFCO_2$ at subcontinental scales. However, because $FFCO_2$ tracers are subject to the same atmospheric transport-related errors that hinder detectability (see next section), as well as other elements (e.g., emissions factors and measurement errors), their use therefore requires further study.

4.4. Effect of Transport and Associated Uncertainties on Detectability

The impact of atmospheric transport-related errors is evaluated by comparing case studies with and without simulated atmospheric transport model errors. By comparing SD_ØFØ with SD_ØFE (Figure 2, fourth and fifth rows), simulated atmospheric transport model errors are introduced in the absence of biospheric fluxes and detectability is found to diminish throughout the year. Atmospheric transport-related errors reduce detectability in the fall and winter more severely than in the case where only biospheric fluxes are added (section 4.3). When the confounding factors of biospheric fluxes and atmospheric transport-related errors are combined, SD_BFE versus SD_BFØ (Figure 2, second and third rows), we see a compounding effect with major losses in detectability in spring, summer, and fall. This result indicates that atmospheric transport-related errors combined with the interference of biospheric fluxes act to amplify the losses in $FFCO_2$ emissions detection.

As realistic errors will likely be more complex than the mean zero, independent, and normally distributed errors added here, the SD_BFE case likely provides an approximate estimate of the impact of atmospheric transport-related errors on detectability. The qualitative similarity between the SD_BFE and RD_BFE cases (section 4.2) shows that the simplified representation of atmospheric transport model errors used here can nevertheless provide information about the overall impact of atmospheric transport-related errors on detectability. Looking ahead, therefore, reducing uncertainty associated with atmospheric transport modeling will be critical to improving the ability to detect, and ultimately quantify, $FFCO_2$ emissions for a majority of the year across nearly all of North America.

An additional case study was designed to explore the impact of seasonal variations in the sensitivity of measurements to underlying fluxes. A lower sensitivity of observations to underlying fluxes is found during the summer relative to winter (Figures S1 and S2, H_{daily} line), due to mixing in a deeper planetary boundary layer and/or stronger convention. To examine the seasonal variation in measurement sensitivity, the underlying fluxes were shifted by 6 months, and thus, summer fluxes occur under winter atmospheric transport conditions and vice versa. Results indicate that the detectability of summertime $FFCO_2$ emissions increases when coupled with wintertime atmospheric transport patterns (results not shown). This suggests that the lack of detectability seen in the summer is in fact due to the compounding effects of not only biospheric fluxes and atmospheric transport-related errors, but also the reduced sensitivity of observations to fluxes during the summer. Conceptually, this result confirms that increasing the sensitivity of the atmospheric observations, through the addition of new measurement sites sensitive to areas with $FFCO_2$ emissions, would improve the detectability of $FFCO_2$ emissions.

These results highlight how the confluence of transport-related issues, interference from the biospheric signal, and reduced sensitivity and number of atmospheric observations (Figure S2) affect the spring, summer, and fall months most strongly, making $FFCO_2$ emissions detectability especially challenging during those seasons.

5. Conclusions and Steps Forward

This paper explores the ability to attribute the variability in high-frequency atmospheric observations to patterns consistent with $FFCO_2$ emissions from subcontinental regions. Results show that the detection of $FFCO_2$ emissions from these regions using in situ CO_2 observations is quite difficult for large portions of the year for NA, a relatively well-monitored continent. Consequently, the use of atmospheric measurements in an inverse

©2014. The Authors.

modeling framework to quantify subcontinental and monthly $FFCO_2$ emissions will pose a significant challenge during spring, summer, and fall months, especially if attempted in areas with less instrumentation than NA.

We identify the interference from biospheric fluxes as specifically hindering $FFCO_2$ emissions detectability during the height of the growing season, while transport-related errors hamper detectability throughout the year. However, detectability of $FFCO_2$ emissions patterns from subcontinental regions is most severely hampered when transport-related errors are exacerbated by a strong biospheric signal. These findings further highlight the need for improved transport model accuracy and an improved monitoring network for $FFCO_2$ emissions.

Nevertheless, we do find that even without the improvements suggested by *Pacala et al*. [2010], the patterns in $FFCO_2$ emissions are detectable for certain regions and certain times of the year. The winter months show reasonable detectability for much of the continental U.S. using the 2008 measurement network. Additionally, $FFCO_2$ emissions are detectable more often in well-instrumented regions (Midwestern U.S., Northeastern U.S., and California and Southwest U.S. regions) in the spring and fall compared to other regions of NA. Well-instrumented regions during nonsummer months offer the most promising opportunity for detecting and subsequently estimating the $FFCO_2$ emissions signal using independent atmospheric observation-based approaches.

Monitoring network design studies [e.g., *Shiga et al*., 2013] tailored toward $FFCO_2$ emissions, could inform the requirements for a network to specifically monitor $FFCO_2$ emissions for subcontinental regions. Providing estimates of $FFCO_2$ emissions based on an atmospheric CO_2 data constraint will ultimately be a challenge with a complex set of solutions. Examining $FFCO_2$ emissions at finer-spatial resolutions by focusing on large emitting urban areas will no doubt provide vital information toward that solution. Measurements of coemitted tracers for $FFCO_2$ [e.g., *Miller et al*., 2012] may also provide an additional observational constraint, analogous to the SD_ØFE case; however, detectability may still be hindered by transport-related errors as well as measurement errors (which can be large for isotopic measurements) and errors in estimating emissions factors. There is also room for methodological improvements within the inverse modeling framework to account for the unique spatiotemporal structure of $FFCO_2$ emissions. Exploring a complementary suite of approaches to the solution to the $FFCO_2$ emissions estimation problem is therefore crucial.

Acknowledgments

This manuscript is based upon work supported by the National Aeronautics and Space Administration under grants NNX12A890G and NNX12AM97G. The authors would like to acknowledge Abhishek Chatterjee, Dorit Hammerling, Deborah Huntzinger, and Yuanyuan Fang for their invaluable expertise, patience, and assistance; the various data providers for the continuous in situ CO_2 data; and Thomas Nehrkorn, John Henderson, and Janusz Eluszkiewicz for completing the WRF simulations.

The Editor thanks two anonymous reviewers for their assistance in evaluating this paper.

References

Andres, R. J., J. S. Gregg, L. Losey, G. Marland, and T. A. Boden (2011), Monthly, global emissions of carbon dioxide from fossil fuel consumption, *Tellus Ser. B Chem. Phys. Meteorol.*, *63*(3), 309–327, doi:10.1111/j.1600-0889.2011.00530.x.

Duren, R. M., and C. E. Miller (2012), Measuring the carbon emissions of megacities, *Nat. Clim. Change*, *2*(8), 560–562, doi:10.1038/nclimate1629.

Gourdji, S. M., et al. (2012), North American CO_2 exchange: Inter-comparison of modeled estimates with results from a fine-scale atmospheric inversion, *Biogeosciences*, *9*(1), 457–475, doi:10.5194/bg-9-457-2012.

Guan, D., Z. Liu, Y. Geng, S. Lindner, and K. Hubacek (2012), The gigatonne gap in China's carbon dioxide inventories, *Nat. Clim. Change*, *2*(9), 672–675, doi:10.1038/nclimate1560.

Gurney, K. R., Y.-H. Chen, T. Maki, S. R. Kawa, A. Andrews, and Z. Zhu (2005), Sensitivity of atmospheric CO_2 inversions to seasonal and interannual variations in fossil fuel emissions, *J. Geophys. Res.*, *110*, D10308, doi:10.1029/2004JD005373.

Gurney, K. R., D. L. Mendoza, Y. Zhou, M. L. Fischer, C. C. Miller, S. Geethakumar, and S. de la Rue du Can (2009), High resolution fossil fuel combustion CO_2 emission fluxes for the United States, *Environ. Sci. Technol.*, *43*(14), 5535–5541, doi:10.1021/es900806c.

Gurney, K. R., I. Razlivanov, Y. Song, Y. Zhou, B. Benes, and M. Abdul-Massih (2012), Quantification of fossil fuel CO_2 emissions on the building/street scale for a large U.S. city, *Environ. Sci. Technol.*, *46*(21), 12,194–12,202, doi:10.1021/es3011282.

Kort, E. A., C. Frankenberg, C. E. Miller, and T. Oda (2012), Space-based observations of megacity carbon dioxide, *Geophys. Res. Lett.*, *39*, L17806, doi:10.1029/2012GL052738.

Lin, J. C., C. Gerbig, S. C. Wofsy, A. E. Andrews, B. C. Daube, K. J. Davis, and C. A. Grainger (2003), A near-field tool for simulating the upstream influence of atmospheric observations: The Stochastic Time-Inverted Lagrangian Transport (STILT) model, *J. Geophys. Res.*, *108*(D16), 4493, doi:10.1029/2002JD003161.

Marland, G. (2008), Uncertainties in accounting for CO_2 from fossil fuels, *J. Ind. Ecol.*, *12*(2), 136–139, doi:10.1111/j.1530-9290.2008.00014.x.

Michalak, A. M., L. Bruhwiler, and P. P. Tans (2004), A geostatistical approach to surface flux estimation of atmospheric trace gases, *J. Geophys. Res.*, *109*, D14109, doi:10.1029/2003JD004422.

Miller, J. B., et al. (2012), Linking emissions of fossil fuel CO_2 and other anthropogenic trace gases using atmospheric $^{14}CO_2$, *J. Geophys. Res.*, *117*, D08302, doi:10.1029/2011JD017048.

Mueller, K. L., V. Yadav, P. S. Curtis, C. Vogel, and A. M. Michalak (2010), Attributing the variability of eddy-covariance CO_2 flux measurements across temporal scales using geostatistical regression for a mixed northern hardwood forest, *Global Biogeochem. Cycles*, *24*, GB3023, doi:10.1029/2009GB003642.

Nassar, R., L. Napier-Linton, K. R. Gurney, R. J. Andres, T. Oda, F. R. Vogel, and F. Deng (2013), Improving the temporal and spatial distribution of CO_2 emissions from global fossil fuel emission data sets, *J. Geophys. Res. Atmos.*, *118*, 917–933, doi:10.1029/2012JD018196.

©2014. The Authors.

Oda, T., and S. Maksyutov (2011), A very high-resolution (1 km × 1 km) global fossil fuel CO_2 emission inventory derived using a point source database and satellite observations of nighttime lights, *Atmos. Chem. Phys.*, *11*(2), 543–556, doi:10.5194/acp-11-543-2011.

Pacala, S., et al. (2010), *Verifying Greenhouse Gas Emissions: Methods to Support International Climate Agreements. Committee on Methods for Estimating Greenhouse Gas Emissions, National Research Council Report*, The National Academies Press, Washington, D. C.

Peylin, P., et al. (2011), Importance of fossil fuel emission uncertainties over Europe for CO(2) modeling: Model intercomparison, *Atmos. Chem. Phys.*, *11*(13), 6607–6622, doi:10.5194/acp-11-6607-2011.

Randerson, J. T., M. V. Thompson, T. J. Conway, I. Y. Fung, and C. B. Field (1997), The contribution of terrestrial sources and sinks to trends in the seasonal cycle of atmospheric carbon dioxide, *Global Biogeochem. Cycles*, *11*, 535, doi:10.1029/97GB02268.

Rayner, P. J., M. R. Raupach, M. Paget, P. Peylin, and E. Koffi (2010), A new global gridded data set of CO_2 emissions from fossil fuel combustion: Methodology and evaluation, *J. Geophys. Res.*, *115*, D19306, doi:10.1029/2009JD013439.

Schwarz, G. (1978), Estimating the dimension of a model, *Ann. Stat.*, *6*(2), 461–464.

Shiga, Y. P., A. M. Michalak, S. Randolph Kawa, and R. J. Engelen (2013), In-situ CO_2 monitoring network evaluation and design: A criterion based on atmospheric CO_2 variability, *J. Geophys. Res. Atmos.*, *118*, 2007–2018, doi:10.1002/jgrd.50168.

Skamarock, W. C., and J. B. Klemp (2008), A time-split nonhydrostatic atmospheric model for weather research and forecasting applications, *J. Comput. Phys.*, *227*(7), 3465–3485, doi:10.1016/j.jcp.2007.01.037.

Turnbull, J., J. Miller, S. Lehman, P. Tans, R. Sparks, and J. Southon (2006), Comparison of (CO_2)-C-14, CO, and SF6 as tracers for recently added fossil fuel CO_2 in the atmosphere and implications for biological CO_2 exchange, *Geophys. Res. Lett.*, *33*, L01817, doi:10.1029/2005GL024213.

Turnbull, J. C., et al. (2011), Assessment of fossil fuel carbon dioxide and other anthropogenic trace gas emissions from airborne measurements over Sacramento, California in spring 2009, *Atmos. Chem. Phys.*, *11*(2), 705–721, doi:10.5194/acp-11-705-2011.

Van der Werf, G. R., J. T. Randerson, L. Giglio, G. J. Collatz, P. S. Kasibhatla, and A. F. Arellano Jr. (2006), Interannual variability in global biomass burning emissions from 1997 to 2004, *Atmos. Chem. Phys.*, *6*, 3423–3441.

Ward, E. J. (2008), A review and comparison of four commonly used Bayesian and maximum likelihood model selection tools, *Ecol. Modell.*, *211*(1–2), 1–10, doi:10.1016/j.ecolmodel.2007.10.030.

©2014. The Authors.